Received: 6 August 2022 | Revised: 6 October 2023 | Accepted: 12 February 2024

DOI: 10.33012/navi.640

ORIGINAL ARTICLE

Synthesized Binary Offset Carrier Modulation for Interoperable GNSS L1 Band Signals

Dhaval J. Upadhyay*[1] | Vijay S. Bhadouria[1] | Parimal J. Majithiya[1] | Subhash C. Bera[1]

[1] Space Applications Centre, Indian Space Research Organisation, Ahmedabad, Gujarat, India

Correspondence
*Dhaval J. Upadhyay
Email: djupadhyay@sac.isro.gov.in

Abstract

This paper presents a constant-envelope modulation scheme, based on a synthesized binary offset carrier (SBOC), for a global navigation satellite system (GNSS) that combines three signals in a nonlinear fashion with unequal amplitudes. The proposed SBOC modulation meets the power spectral density criteria of multiplexed binary offset carrier (MBOC) modulation used in the L1 frequency band (1575.42 MHz) open civilian service interoperable signals for GNSS. This SBOC modulation also allows for the selection of an arbitrary power-sharing ratio between the data and pilot signals. This approach provides better performance than various MBOC(6, 1, 1⁄11) modulations for narrowband receivers.

Keywords

constant envelope, GNSS, interoperable, MBOC

1 | INTRODUCTION

Many global navigation satellite system (GNSS) service providers plan to provide interoperable open civilian service in the L1 frequency band (1575.42 MHz). Hence, service providers have defined multiplexed binary offset carrier (MBOC) modulation for the L1 frequency band interoperable open civilian service (Hein et al., 2006). The prime goal in designing an interoperable open civilian signal in the L1 frequency band is to design a navigation signal that satisfies the power spectral density (PSD) requirement of MBOC(6, 1, 1⁄11) modulation (Hein et al., 2006). The PSD of the MBOC(6, 1, 1⁄11) modulation signal ($S_{MBOC(6,1,1/11)}(f)$) is defined as follows:

$$\begin{aligned} S_{MBOC(6,1,1/11)}(f) &= \frac{10}{11}S_{BOC(1,1)}(f) + \frac{1}{11}S_{BOC(6,1)}(f) \\ &= \frac{10\sin^2(\pi f T_c)\sin^2\left(\frac{\pi f T_c}{2}\right)}{11T_c\left(\pi f \cos\left(\frac{\pi f T_c}{2}\right)\right)^2} + \frac{\sin^2(\pi f T_c)\sin^2\left(\frac{\pi f T_c}{12}\right)}{11T_c\left(\pi f \cos\left(\frac{\pi f T_c}{12}\right)\right)^2} \end{aligned} \quad (1)$$

The MBOC modulation contains binary offset carrier (BOC) (1,1) and BOC(6,1) components with 10⁄11 and 1⁄11 power sharing, respectively.

[0]**Abbreviations:** MBOC, multiplexed binary offset carrier

GNSS service providers have proposed various methods for implementing MBOC modulation, such as time-multiplexed BOC (TMBOC), composite BOC (CBOC), and quadrature multiplexed BOC (QMBOC), to meet the MBOC(6, 1, 1/11) PSD criteria (Avila-Rodriguez et al., 2008; Betz et al., 2006; Yao, Lu, & Feng, 2010). The Global Positioning System uses the TMBOC implementation method, which combines the BOC(1,1) and BOC(6,1) components in a time-multiplexing manner (Betz et al., 2006). Galileo uses the CBOC implementation method, which combines the BOC(1,1) and BOC(6,1) components in a baseband level with desired amplitude factors (Avila-Rodriguez et al., 2008). BeiDou uses the QMBOC implementation method, which the combines BOC(1,1) and BOC(6,1) components in a quadrature multiplexing manner with desired amplitude factors (Yao, Lu, & Feng, 2010). CBOC does not provide flexibility in allocating the power-sharing of data and pilot signals because of the cross-product terms between the BOC(1,1) and BOC(6,1) components of the data and pilot signals in the autocorrelation of these signals (Avila-Rodriguez et al., 2008). Allocating equal power to the CBOC data and pilot signals removes these cross-product terms in the autocorrelation of the CBOC signal. TMBOC and QMBOC provide flexibility in allocating power-sharing between data and pilot signals. Typically, these MBOC modulation signals are multiplexed onboard a satellite with another open civilian service, public regulated services, and restricted service signals in order to generate a constant-envelope modulus composite signal (Avila-Rodriguez et al., 2008; Yao et al., 2017; Yao & Lu, 2021). A constant-envelope modulus composite signal enables the operation of an onboard high-power amplifier in a saturation region, providing maximum efficiency. However, all of these MBOC implementation methods are based on non-constant-envelope modulus signals when GNSS satellites transmit only the L1 frequency band interoperable open civilian service signal, corresponding to standalone transmission of the MBOC-modulated signal.

2 | SYNTHESIZED BINARY OFFSET CARRIER (SBOC) MODULATION

In general, a baseband spread-spectrum signal $s(t)$ is represented as follows:

$$s(t) = \sum_{n=-\infty}^{\infty} (-1)^{c_n} p(t - nT_c) \tag{2}$$

where c_n is the spreading code, $p(t)$ is the spreading chip waveform, which is nonzero within the interval of $[0, T_c)$, and T_c is the chip interval. For a step-shaped coded symbol (SCS) signal with a modulation subcarrier interval of T_s, where $T_s \le T_c$, the spreading chip waveform is represented by the following:

$$p(t) = \sum_{k=0}^{M-1} \psi_k(t) \kappa_k \tag{3}$$

Here, M is the modulation index of the waveform representing the number of half-cycles of the subcarrier within the chip interval, i.e., $M = \frac{2T_c}{T_s}$, and $\psi_k(t)$ is the basis signal of the spreading waveform, given as follows:

$$\psi_k(t) = \begin{cases} \frac{1}{\sqrt{T_c}}, & kT_s \le t < (k+1)T_s \\ 0, & \text{otherwise} \end{cases} \tag{4}$$

Here, κ_k is the shape vector that characterizes the spreading waveform, which is given by the following:

$$\kappa_k = M \int_0^{T_c} p(t)\psi_k(t)dt \tag{5}$$

The SCS signal $s(t)$ is periodic with the chip interval T_c. Hence, for a given value of T_c and T_s, the signal $s(t)$ is completely characterized by the shape vector $\kappa_k = [\kappa_1, \kappa_2, \ldots, \kappa_{M-1}]^T$ and is represented in parameterized form as follows:

$$s(t;\kappa) = \sum_{n=-\infty}^{\infty} \sum_{k=0}^{M-1} (-1)^{c_n} \kappa_k \psi_k(t - nMT_s) \tag{6}$$

For a BOC-type signal of the type $BOC(m,n)$, where $M = \frac{2m}{n}$ and m is an integer multiple of n, the shape vector κ_k is given by the following:

$$\kappa_k = (-1)^k \,|_{k\in[0,\ldots,M-1]} \tag{7}$$

In this paper, we propose a constant-envelope modulation method that combines three signals: the BOC(1,1) and BOC(6,1) components of the pilot signal and the BOC(1,1) component of the data signal. These signals are combined in a nonlinear fashion with unequal amplitudes. The proposed method generates a fourth signal, the BOC(6,1) component of the data signal, by multiplexing these three signals. The proposed method synthesizes four signals with unequal amplitudes to generate SBOC modulation (Upadhyay & Bhadouria, 2021; Upadhyay et al., 2020). Figure 1 shows the SBOC modulation generation method. We represent the shape vectors of the data and pilot components of the SBOC signal as κ_k^p and κ_k^d, respectively, which are defined as follows:

$$\kappa_k^p = \sqrt{\alpha}\kappa_k^1 - \sqrt{\beta}\kappa_k^2 \tag{8}$$

$$\kappa_k^d = \sqrt{\gamma}\kappa_k^1 + g(\alpha,\beta,\gamma)\kappa_k^2 \tag{9}$$

where $\kappa_k^1 = (-1)^{\left\lfloor \frac{k}{6} \right\rfloor}$ is the shape vector of BOC(1,1), $\kappa_k^2 = (-1)^k$ is the shape vector of BOC(6,1), and $\lfloor . \rfloor$ represents the floor operation. We represent a general $SBOC$ signal $(s_{SBOC}(t))$ with the PSD given in Equation (1) in terms of the pilot signal $(s^p(t;\kappa^p))$ and data signal $(s^d(t;\kappa^d))$ as follows:

$$s_{SBOC}(t) = s^p(t;\kappa^p) + j\, s^d(t;\kappa^d) \tag{10}$$

Here, both the data and pilot signals are the combination of BOC(1,1) with modulation index $M_{BOC(1,1)} = 2$ and BOC(6,1) with modulation index $M_{BOC(6,1)} = 12$, represented as follows:

$$s^p(t;\kappa^p) = \sqrt{\alpha}s^p_{BOC(1,1)}(t) - \sqrt{\beta}s^p_{BOC(6,1)}(t) \tag{11}$$

$$s^d(t;\kappa^d) = \sqrt{\gamma}s^d_{BOC(1,1)}(t) + f(t;\alpha,\beta,\gamma) \tag{12}$$

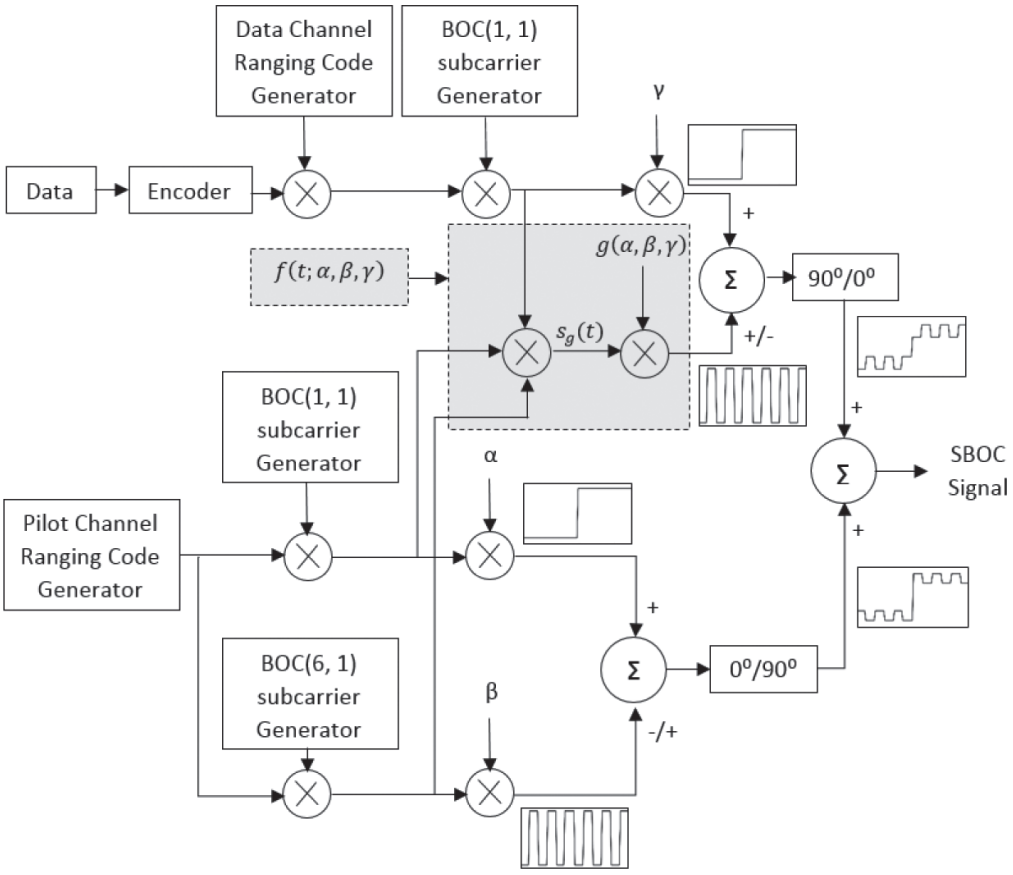

FIGURE 1 SBOC modulation generation method

where the notation $(x)_{BOC(m,n)}$ represents the $BOC(m,n)$ component of the signal x and α, β, and γ are parameters that control the PSD of $s_{SBOC}(t)$. Mapping $f(t;\alpha,\beta,\gamma)$ controls both the PSD and the envelope of $s_{SBOC}(t)$, which is represented as follows:

$$f(t;\alpha,\beta,\gamma) = g(\alpha,\beta,\gamma)s_g(t) \tag{13}$$

where $s_g(t)$ is generated by multiplexing the $s^p_{BOC(1,1)}(t)$, $s^p_{BOC(6,1)}(t)$, and $s^d_{BOC(1,1)}(t)$ signals, as follows:

$$\begin{aligned} s_g(t) &= s^p_{BOC(1,1)}(t)s^p_{BOC(6,1)}(t)s^d_{BOC(1,1)}(t) \\ &= s^d_{BOC(6,1)}(t) \end{aligned} \tag{14}$$

Considering Equations (6), (7), and (13), Equations (11) and (12) can be written in terms of the SCS signal as follows:

$$\begin{aligned} s^p(t;\kappa^p) &= \sqrt{\alpha}\sum_{n=-\infty}^{\infty}\sum_{k=0}^{M-1}(-1)^{c^p_n}(-1)^{\left\lfloor \frac{M_{BOC(1,1)}k}{M}\right\rfloor}\psi_k(t-nMT_s) \\ &\quad + \sqrt{\beta}\sum_{n=-\infty}^{\infty}\sum_{k=0}^{M-1}(-1)^{c^p_n}(-1)^{\left\lfloor \frac{M_{BOC(6,1)}k}{M}\right\rfloor+1}\psi_k(t-nMT_s) \\ &= \sum_{n=-\infty}^{\infty}\sum_{k=0}^{M-1}(-1)^{c^p_n}\kappa^p_k\psi_k(t-nMT_s) \end{aligned} \tag{15}$$

$$s^d(t;\kappa^d) = \sqrt{\gamma}\sum_{n=-\infty}^{\infty}\sum_{k=0}^{M-1}(-1)^{c_n^d}(-1)^{\left\lfloor \frac{M_{BOC(1,1)}k}{M}\right\rfloor}\psi_k(t-nMT_s) + g(\alpha,\beta,\gamma)\sum_{n=-\infty}^{\infty}\sum_{k=0}^{M-1}(-1)^{c_n^d}(-1)^{\left\lfloor \frac{M_{BOC(6,1)}k}{M}\right\rfloor}\psi_k(t-nMT_s) = \sum_{n=-\infty}^{\infty}\sum_{k=0}^{M-1}(-1)^{c_n^d}\kappa_k^d\psi_k(t-nMT_s) \quad (16)$$

where c_n^p and c_n^d are the code-division multiple access ranging codes for the pilot and data signals, respectively, which are assumed to be mutually orthogonal. T_s is the sub-chip interval given by $T_s = T_c/M$, T_c is the code chip duration, and $M = LCM(M_{BOC(1,1)}, M_{BOC(6,1)}) = 12$ is the modulation index of the data and pilot component of the SBOC signal. Equation (16) does not show the data component without a loss of generality.

To meet both the $S_{MBOC(6,1,1/11)}(f)$ PSD and constant-envelope requirements, the value of $g(\alpha,\beta,\gamma)$ is obtained by solving the following equations:

$$\alpha+\beta+\gamma+g(\alpha,\beta,\gamma)^2 = 1 \quad (17)$$

$$\beta+g(\alpha,\beta,\gamma)^2 = 1/11 \quad (18)$$

$$\alpha+\gamma = 10/11 \quad (19)$$

$$\sqrt{(\kappa_k^d)^2+(\kappa_k^p)^2} = 1|_{k\in[0,\ldots,M-1]} \quad (20)$$

Here, $g(\alpha,\beta,\gamma) = \sqrt{\frac{\alpha\beta}{\gamma}}$; a corresponding proof is given in Lemma 1.

Lemma 1. The envelope of $s_{SBOC}(t)$ is always constant for all values of α, β, and γ.

Proof. Because any periodic spread-spectrum signal of SCS form is completely characterized by its shape vector κ, without a loss of generality, the minimum value of the envelope of $s_{SBOC}(t)$ is given by the following:

$$\min_k |s_{SBOC}(t)| = \sqrt{(\sqrt{\alpha}-\sqrt{\beta})^2+(\sqrt{\gamma}+g(\alpha,\beta,\gamma))^2} = \sqrt{\alpha+\beta+\gamma+g(\alpha,\beta,\gamma)^2-2\sqrt{\alpha\beta}+2\sqrt{\gamma}g(\alpha,\beta,\gamma)} = \sqrt{1-2\sqrt{\alpha\beta}+2\sqrt{\gamma}g(\alpha,\beta,\gamma)} = 1 \quad (21)$$

By solving Equation (21), we obtain $g(\alpha,\beta,\gamma) = \sqrt{\frac{\alpha\beta}{\gamma}}$. Similarly, by using $g(\alpha,\beta,\gamma) = \sqrt{\frac{\alpha\beta}{\gamma}}$, it can be shown that $\max_k |s_{SBOC}(t)| = 1$. Hence, we have proven that $|s_{SBOC}(t)| = 1$. □

Lemma 2. The PSD of $S_{SBOC}(f)$ is equivalent to the PSD of the MBOC modulation $S_{MBOC(6,1,1/11)}(f)$.

Proof. By using Equation (10) and assuming $\mathbb{E}(s^p(t;\kappa^p)) = \mathbb{E}(s^d(t;\kappa^d)) = 0$ and orthogonal codes on the data and pilot signals, i.e., $\mathbb{E}(c_n^p c_m^d) = 0$, we obtain the following:

$$\mathbb{E}(s_{SBOC}(t-\tau)^* s_{SBOC}(t)) = \mathcal{R}_{s_{SBOC}}(\tau) = \mathbb{E}(s^p(t-\tau;\kappa_k^p)^* s^p(t;\kappa_k^p)) + \mathbb{E}(s^d(t-\tau;\kappa_k^d)^* s^d(t;\kappa_k^d)) \quad (22)$$

By applying Equations (11) and (12), we obtain the following:

$$\begin{aligned}\mathcal{R}_{s_{S\,BOC}}(\tau) &= \alpha\,\mathbb{E}(s^p(t-\tau;\kappa_k^1)^* s^p(t;\kappa_k^1)) + \beta\,\mathbb{E}(s^p(t-\tau;\kappa_k^2)^* s^p(t;\kappa_k^2)) \\ &\quad - 2\sqrt{\alpha\beta}\,\mathbb{E}(s^p(t-\tau;\kappa_k^1)^* s^p(t;\kappa_k^2)) + \gamma\,\mathbb{E}(s^d(t-\tau;\kappa_k^1)^* s^d(t;\kappa_k^1)) \\ &\quad + \frac{\alpha\beta}{\gamma}\,\mathbb{E}(s^d(t-\tau;\kappa_k^2)^* s^d(t;\kappa_k^2)) + 2\sqrt{\alpha\beta}\,\mathbb{E}(s^d(t-\tau;\kappa_k^1)^* s^d(t;\kappa_k^2))\end{aligned} \tag{23}$$

By considering the data and the pilot channel code to have identical statistical characteristics, i.e., $\mathbb{E}(s^p(t-\tau;\kappa_k^1)^* s^p(t;\kappa_k^1)) = \mathbb{E}(s^d(t-\tau;\kappa_k^1)^* s^d(t;\kappa_k^1)) = \mathcal{R}_{\kappa_k^1}(\tau)$, $\mathbb{E}(s^p(t-\tau;\kappa_k^2)^* s^p(t;\kappa_k^2)) = \mathbb{E}(s^d(t-\tau;\kappa_k^2)^* s^d(t;\kappa_k^2)) = \mathcal{R}_{\kappa_k^2}(\tau)$ and $\mathbb{E}(s^p(t-\tau;\kappa_k^1)^* s^p(t;\kappa_k^2)) = \mathbb{E}(s^d(t-\tau;\kappa_k^1)^* s^d(t;\kappa_k^2))$, we obtain the following:

$$\mathcal{R}_{s_{S\,BOC}}(\tau) = (\alpha+\gamma)\mathcal{R}_{\kappa_k^1}(\tau) + \left(\beta + \frac{\alpha\beta}{\gamma}\right)\mathcal{R}_{\kappa_k^2}(\tau) \tag{24}$$

where $\mathcal{R}_{\kappa_k^1}(\tau)$ and $\mathcal{R}_{\kappa_k^2}(\tau)$ are calculated as reported by Yao, Cui, et al. (2010) and Yao & Lu (2021) as follows:

$$\begin{aligned}\mathcal{R}_{\kappa_k^1}(\tau) &= \frac{1}{T}\int_0^T s^p(t-\tau;\kappa_k^1)^* s^p(t;\kappa_k^1)dt \\ &= \frac{1}{T}\sum_{n=-\infty}^{\infty}\sum_{m=-\infty}^{\infty}\sum_{k=0}^{M-1}\sum_{q=0}^{M-1}(-1)^{c_n^p+c_m^p}\kappa_k^1\kappa_q^1\int_0^T \psi_k(t-mMT_s)\psi_q(t-nMT_s-\tau)dt\end{aligned} \tag{25}$$

Here, $T = NT_c$ is the period of the spreading code. For a sufficiently large spreading code period, it can be assumed that the autocorrelation property of the spreading code is ideal, i.e., $R_a \triangleq \frac{1}{N}\sum_{n=0}^{N-1}(-1)^{c_n^p+c_{a+n}^p} = 1$ for $a = 0$. The integral term in Equation (25) is nonzero only when $\psi_k(t-mMT_s)$ and $\psi_q(t-nMT_s-\tau)$ overlap, i.e., $|(k-q)T_s+\tau| < T_s$ within the chip duration $T_c(N=1)$. Hence, τ can be expressed as $\tau = bT_s + \epsilon$, where $b \in [0, M-1]$ and $\epsilon \in [0, T_s)$. Furthermore, using these expressions, we can rewrite the integral term given in Equation (25) as follows:

$$\frac{1}{T_s}\int_{\epsilon}^{T_s}\psi_k(t)\psi_k(t-\epsilon)dt = 1 - \frac{\epsilon}{T_s} \tag{26}$$

$$\frac{1}{T_s}\int_{T_s-\epsilon}^{T_s}\psi_k(t)\psi_k(t-\epsilon)dt = \frac{\epsilon}{T_s} \tag{27}$$

We can rewrite Equation (25) as follows:

$$\begin{aligned}\mathcal{R}_{\kappa_k^1}(\tau) = \frac{1}{M}\Bigg[&\sum_{k=0}^{M-1}\kappa_k^1\kappa_{b+k}^1\left(1-\frac{\epsilon}{T_s}\right) + \sum_{k=0}^{M-1}\kappa_k^1\kappa_{b+k+1}^1\left(\frac{\epsilon}{T_s}\right) \\ &+ \sum_{k=0}^{M-1}\kappa_k^1\kappa_{b+k-M}^1\left(1-\frac{\epsilon}{T_s}\right) + \sum_{k=0}^{M-1}\kappa_k^1\kappa_{b+k-M+1}^1\left(\frac{\epsilon}{T_s}\right)\Bigg]\end{aligned} \tag{28}$$

We define r_b^1 as follows:

$$r_b^1 \triangleq \frac{1}{M}\sum_{k=0}^{M-1}\kappa_k^1\kappa_{b+k}^1 \tag{29}$$

Substituting Equation (29) in Equation (28), we obtain the following:

$$\begin{aligned}\mathcal{R}_{\kappa_k^1}(\tau) &= r_b^1\left(1-\frac{\epsilon}{T_s}\right)+r_{b+1}^1\left(\frac{\epsilon}{T_s}\right)+r_{b-M}^1\left(1-\frac{\epsilon}{T_s}\right)+r_{b-M+1}^1\left(\frac{\epsilon}{T_s}\right)\\ &=\left(1-\frac{\epsilon}{T_s}\right)\left[r_b^1+r_{b-M}^1\right]+\left(\frac{\epsilon}{T_s}\right)\left[r_{b+1}^1+r_{b-M+1}^1\right],\ |\tau|<T_c\end{aligned} \tag{30}$$

Similarly, we have the following:

$$\mathcal{R}_{\kappa_k^2}(\tau)=\left(1-\frac{\epsilon}{T_s}\right)\left[r_b^2+r_{b-M}^2\right]+\left(\frac{\epsilon}{T_s}\right)\left[r_{b+1}^2+r_{b-M+1}^2\right],\ |\tau|<T_c \tag{31}$$

where r_b^2 is defined as follows:

$$r_b^2 \triangleq \frac{1}{M}\sum_{k=0}^{M-1}\kappa_k^2\kappa_{b+k}^2 \tag{32}$$

Substituting Equations (18) and (19) in Equation (24), we obtain the following:

$$\begin{aligned}\mathcal{R}_{s_{SBOC}}(\tau) &= (\alpha+\gamma)\mathcal{R}_{\kappa_k^1}(\tau)+\left(\beta+\frac{\alpha\beta}{\gamma}\right)\mathcal{R}_{\kappa_k^2}(\tau)\\ &=(\alpha+\gamma)\mathcal{R}_{\kappa_k^1}(\tau)+(\beta+(g(\alpha,\beta,\gamma))^2))\mathcal{R}_{\kappa_k^2}(\tau)\\ &=\frac{10}{11}\mathcal{R}_{\kappa_k^1}(\tau)+\frac{1}{11}\mathcal{R}_{\kappa_k^2}(\tau)\end{aligned} \tag{33}$$

We obtain the PSD of a cyclostationary process using the Wiener–Khinchin theorem (Yao & Lu, 2021):

$$\begin{aligned}S_{s_{SBOC}}(f) &= \mathcal{F}(\mathcal{R}_{s_{SBOC}}(\tau))\\ &=\frac{10}{11}S_{BOC(1,1)}(f)+\frac{1}{11}S_{BOC(6,1)}(f)\\ &=\frac{10\sin^2(\pi f T_c)\sin^2\left(\frac{\pi f T_c}{2}\right)}{11T_c\left(\pi f\cos\left(\frac{\pi f T_c}{2}\right)\right)^2}+\frac{\sin^2(\pi f T_c)\sin^2\left(\frac{\pi f T_c}{12}\right)}{11T_c\left(\pi f\cos\left(\frac{\pi f T_c}{12}\right)\right)^2}\end{aligned} \tag{34}$$

Hence, we have proven that $S_{s_{SBOC}}(f)=S_{MBOC(6,1,1/11)}(f)$. □

3 | SBOC PERFORMANCE

Table 1 shows flexibility in the selection of power-sharing of the BOC(1,1) and BOC(6,1) components of the data and pilot signals for the SBOC modulation. Typically, high-accuracy receivers, which are wideband, correlate the MBOC-modulated received signal against an exact replica of the MBOC-modulated signal, having both the BOC(1,1) and BOC(6,1) components. These wideband receivers are known as matched receivers. In contrast, low-cost receivers, which are widely used in commercial applications, have a narrow receiver bandwidth. These narrowband receivers correlate the MBOC-modulated received signal against

TABLE 1
SBOC Modulation Data/Pilot Power-Sharing Options

Option	α	β	γ	$\alpha\beta/\gamma$	Data (%)	Pilot (%)
1	4/11	6/110	6/11	4/110	58.18	41.82
2	5/11	5/110	5/11	5/110	50.00	50.00
3	**6/11**	**4/110**	**4/11**	**6/110**	**41.82**	**58.18**
4	7/11	3/110	3/11	7/110	33.64	66.36
5	8/11	2/110	2/11	8/110	25.45	74.55

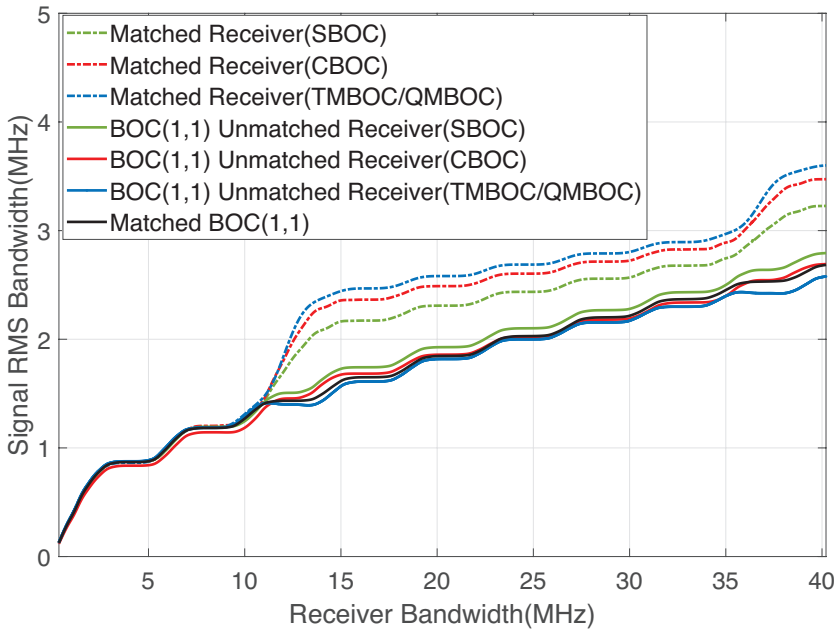

FIGURE 2 RMS bandwidth of the SBOC pilot signal (option 3)

a BOC(1,1) replica rather than a perfect MBOC-modulated signal replica. These receivers are known as unmatched receivers. Thus, the bandwidth of unmatched receivers is typically lower than that of matched receivers. Hence, we propose SBOC power-sharing option 3 to achieve optimum performance for BOC(1,1) unmatched receivers. The major performance metrics of navigation signal designs are the root mean square (RMS) bandwidth, correlation shape, and multipath performance (Avila-Rodriguez et al., 2008; Hein et al., 2006; Yao et al., 2017; Yao & Lu, 2021). The RMS bandwidth quantifies the power content of the signal over the frequencies across its bandwidth. For a signal with a normalized PSD of $G(f)$, the RMS bandwidth of the signal is defined as follows (Yao & Lu, 2021):

$$\beta_{RMS}(B) = \left[\frac{\int_{-B/2}^{B/2} f^2 G(f) df}{\int_{-B/2}^{B/2} G(f) df} \right]^{1/2} \tag{35}$$

where B is the receiver bandwidth. Hence, the RMS bandwidth, correlation shape, and multipath performance of the proposed SBOC modulation are compared with the performance of various MBOC modulations. Figure 2 shows a comparison of the RMS bandwidth of the SBOC (option 3) pilot signal with various MBOC

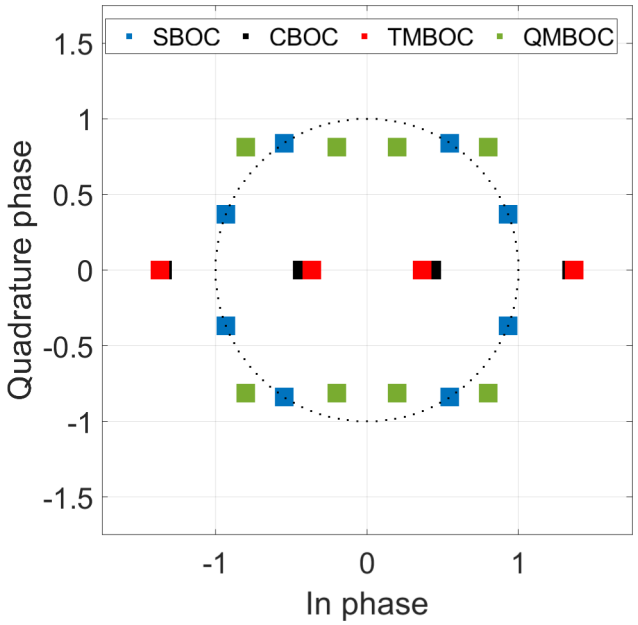

FIGURE 3 Constellation diagram of the SBOC signal (option 3)

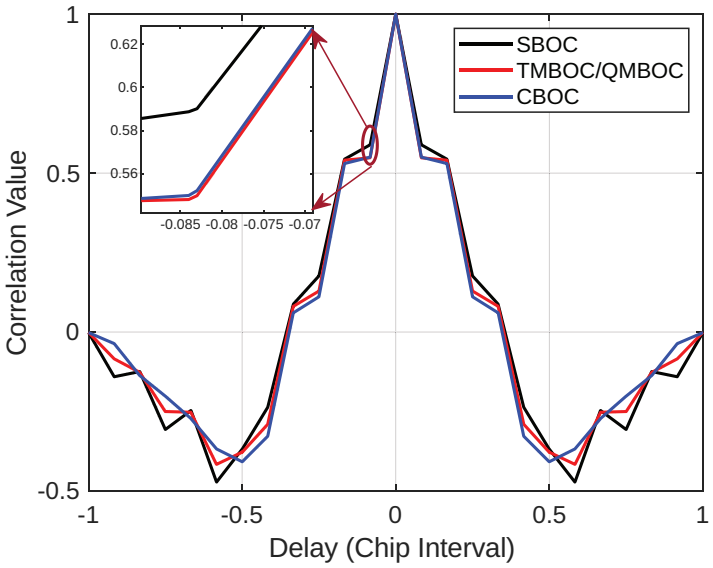

FIGURE 4 Autocorrelation of the pilot signal (option 3)

pilot signals. The SBOC (option 3) pilot signal performs better than various MBOC pilot signals for a BOC(1,1) unmatched receiver because less power is allocated in the BOC(6,1) component of the pilot signal compared with MBOC modulations. Consequently, the SBOC (option 3) pilot signal performs poorer than various MBOC pilot signals for matched receivers.

Figure 3 shows a comparison of the constellation diagram for SBOC (option 3) with various MBOC modulations when they are generated alone without multiplexing with other signals. The results show that the envelope of SBOC modulation is a constant modulus, which enables the operation of an onboard high-power amplifier in the saturation region. Figures 4 and 5 show the autocorrelation and multipath performance (0.1 chip spacing) of the SBOC (option 3) pilot signal,

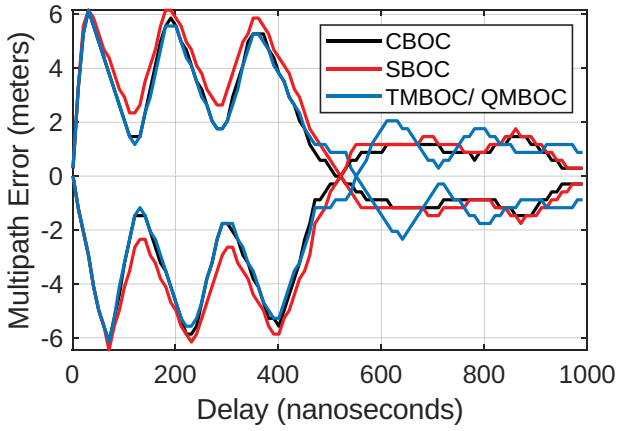

FIGURE 5 Multipath performance of the pilot signal (option 3)

respectively. The autocorrelation peak is slightly wider than that of various MBOC pilot signals, matching the RMS bandwidth performance. The SBOC pilot signal multipath results show ~0.5-m poorer performance than various MBOC pilot signals because of the wider autocorrelation peak.

4 | CONCLUSION

We have proposed a constant-envelope SBOC modulation method for interoperable GNSS L1 band signals that combines three signals in a nonlinear fashion with unequal amplitudes. The proposed SBOC modulation meets the PSD criteria of MBOC(6, 1, 1⁄11) modulations used in the L1 frequency band (1575.42 MHz) open civilian service signals of GNSS and provides better performance than various MBOC(6, 1, 1⁄11) modulations for narrowband receivers. Moreover, this approach also allows for the selection of an arbitrary power-sharing ratio between the data and pilot signals.

ACKNOWLEDGMENTS

The authors are grateful to Shri. Sumitesh Sarkar, Deputy Director, SATCOM and Navigation Payload Area-Space Applications Centre (SAC)-Indian Space Research Organisation (ISRO), Shri. K. S. Parikh, Associate Director, SAC-ISRO, and Shri. Nilesh Desai, Director, SAC-ISRO for their guidance and support.

REFERENCES

Avila-Rodriguez, J.-A., Hein, G. W., Wallner, S., Issler, J.-L., Ries, L., Lestarquit, L., de Latour, A., Godet, J., Bastide, F., Pratt, T., & Owen, J. (2008). The MBOC modulation: The final touch to the Galileo frequency and signal plan. *NAVIGATION*, *55*(1), 15–28. https://doi.org/10.1002/j.2161-4296.2008.tb00415.x

Betz, J., Blanco, M. A., Cahn, C. R., Dafesh, P. A., Hegarty, C. J., Hudnut, K. W., Kasemsri, V., Keegan, R., Kovach, K., Lenahan, L. S., Ma, H. H., Rushanan, J. J., Sklar, D., Stansell, T. A., Wang, C. C., & Yi, S. K. (2006). Description of the L1C signal. *Proc. of the 19th International Technical Meeting of the Satellite Division of the Institute of Navigation (ION GNSS 2006),* Fort Worth, TX, 2080–2091. https://www.ion.org/publications/abstract.cfm?articleID=6891

Hein, G. W., Avila-Rodriguez, J.-A., Wallner, S., Pratt, A. R., Owen, J., Issler, J., Betz, J. W., Hegarty, C. J., Lenahan, S., Rushanan, J. J., Kraay, A. L., & Stansell, T. A. (2006). MBOC: the new optimized spreading modulation recommended for Galileo L1 OS and GPS L1C. *Proc. of the 2006 IEEE/ION Position, Location, and Navigation Symposium (PLANS),* Coronado, CA, 883–892. https://doi.org/10.1109/PLANS.2006.1650688

Upadhyay, D. J., & Bhadouria, V. S. (2021). Overview of new NavIC L1 SPS signal structure & SBOC modulation and modified-CEMIC multiplexing scheme. *Proc. of the 15th Meeting of*

the International Committee on Global Navigation Satellite Systems (ICG), Vienna, Austria. www.unoosa.org/documents/pdf/icg/2021/ICG15/WGS/icg15_wgs_01.pdf

Upadhyay, D. J., Majithiya, P. J., Bhadouria, V. S., & Bera, S. C. (2020). *Method for generating modulation signals for a satellite navigation system*. India Patent 355353.

Yao, Z., Cui, X., Lu, M., Feng, Z., & Yang, J. (2010). Pseudo-correlation-function-based unambiguous tracking technique for sine-BOC signals. *IEEE Transactions on Aerospace and Electronic Systems*, *46*(4), 1782–1796. https://doi.org/10.1109/TAES.2010.5595594

Yao, Z., Guo, F., Ma, J., & Lu, M. (2017). Orthogonality-based generalized multicarrier constant envelope multiplexing for DSSS signals. *IEEE Transactions on Aerospace and Electronic Systems*, *53*(4), 1685–1698. https://doi.org/10.1109/TAES.2017.2671580

Yao, Z., & Lu, M. (2021). *Next-Generation GNSS Signal Design*. Singapore: Springer. https://doi.org/10.1007/978-981-15-5799-6

Yao, Z., Lu, M., & Feng, Z. (2010). Quadrature multiplexed BOC modulation for interoperable GNSS signals. *Electronics letters*, *46*(17), 1234–1236. https://doi.org/10.1049/el.2010.1693

How to cite this article: Upadhyay, D. J., Bhadouria, V. S., Majithiya, P. J., & Bera, S. C. (2024). Synthesized binary offset carrier modulation for interoperable GNSS L1 band signals. *NAVIGATION, 71*(2). https://doi.org/10.33012/navi.640